HERA data and DGLAP evolution

Caola, Fabrizio; Forte, Stefano; Rojo, Juan

published in
Nuclear Physics A
2010

DOI (link to publisher)
10.1016/j.nuclphysa.2010.08.009

IFUM-962-FT

HERA data and DGLAP evolution: theory and phenomenology

Fabrizio Caola, Stefano Forte and Juan Rojo,

Dipartimento di Fisica, Università di Milano and INFN, Sezione di Milano, Via Celoria 16, I-20133 Milano, Italy

Abstract:

We examine critically the evidence for deviations from next-to-leading order perturbative DGLAP evolution in HERA data. We briefly review the status of perturbative small-x resummation and of global determinations of parton distributions. We then show that the geometric scaling properties of HERA data are consistent with DGLAP evolution, which is also strongly supported by the double asymptotic scaling properties of the data. We finally show that backwards evolution of parton distributions into the low x, low Q^2 region shows evidence of deviations between the observed behaviour and the next-to-leading order predictions. These deviations cannot be explained by missing next-to-next-to-leading order perturbative terms, but are consistent with perturbative small-x resummation.

1 DGLAP evolution in the LHC era

Perturbative QCD is a quantitatively tested theory which describes in a very accurate way a vast body of data, and it is at the basis of physics at colliders such as the LHC [1]. The DGLAP equations, i.e. the renormalization-group equations which govern the scale dependence of parton distributions are, together with asymptotic freedom and factorization, a cornerstone of the theory, both in terms of phenomenological success and theoretical foundation. Specifically, they are the tool which allows us to combine information on nucleon structure from a variety of data, and use it for predictions at the LHC.

The current frontier in perturbative QCD is systematically going from the second to the third perturbative order, namely from next-to-leading (NLO) to next-to-next-to-leading order (NNLO). In view of this, it is of utmost importance for both theory and phenomenology to understand whether in any given kinematic region an order-by-order perturbative approach is sufficient. There is now considerable theoretical evidence that at sufficiently high center-of-mass energies this approach may break down, and thus as this region is approached one should resum to all orders perturbative corrections which are logarithmically enhanced in the ratio x of the hard scale to center-of-mass energy — the so–called small-x resummation. However, conclusive experimental evidence for such resummation effects in the data is lacking, partly due to the fact that the relevant effects are difficult to disentangle from model and theoretical assumptions.

It is the purpose of this contribution to review, update and put in context a recent attempt to provide some such evidence. The outline of this contribution is as follows.

In Sect. 2 we briefly review the status of linear small-x resummation. Then in Sect. 3 we present the state of the art of fixed-order DGLAP and global PDF analysis and its implications for the LHC. Finally in Sect. 4 we present a technique designed to identify deviations from NLO DGLAP evolution in the data, and apply it to recent global parton fit. We will specifically see that previous evidence of deviations from NLO DGLAP is considerably strengthened by the recent precise combined HERA-I determination of deep-inelastic structure functions.

2 Small-x resummation

As well known, deep–inelastic partonic cross sections and parton splitting functions receive large corrections in the small-x limit due to the presence of powers of $\alpha_s \log x$ to all orders in the perturbative expansion [2,3]. This suggests dramatic effects from yet higher orders, so the success of NLO perturbation theory at HERA has been for a long time very hard to explain. In the last several years this situation has been clarified [4–9], showing that, once the full resummation procedure accounts for running coupling effects, gluon exchange symmetry and other physical constraints, the effect of the resummation of terms which are enhanced at small-x is perceptible but moderate — comparable in size to typical NNLO fixed order corrections in the HERA region.

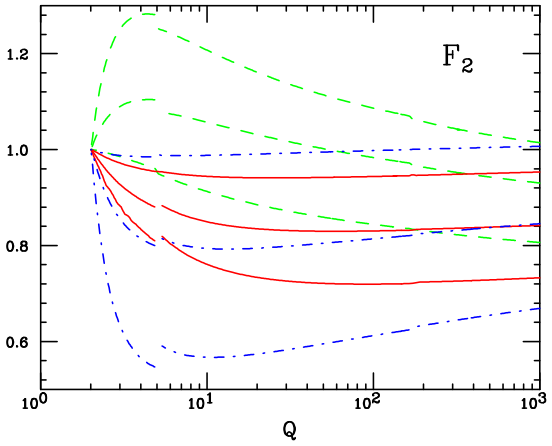

Figure 1: Ratio of the resummed and NNLO prediction to the NLO fixed order for the singlet F_2 deep–inelastic structure function. The curves are: fixed order perturbation theory NNLO (green, dashed); resummed NLO in $Q_0\overline{\rm MS}$ scheme (red, solid), resummed NLO in the $\overline{\rm MS}$ scheme (blue, dot-dashed). In each case, the three curves shown correspond to fixed $x = 10^{-2}$, $x = 10^{-4}$, $x = 10^{-6}$, with the smallest x value showing the largest deviations.

For phenomenology, it is necessary to resum not only evolution equations, but also hard partonic coefficient functions. The relevant all–order coefficients have been computed for DIS [2,3], and more recently for several LHC processes such as heavy quark production [10], Higgs production [11,12], Drell-Yan [13,14] and prompt photon production [15,16]. These coefficients can be used for a full resummation of physical observables, by suitably combining them with resummed DGLAP evolution and accounting for running–coupling effects, so as to maintain perturbative independence of physical observables of the choice of factorization scheme [17].

This program has been carried out for the first time for deep–inelastic scattering in Ref. [6], and more recently for prompt photon production [18], which makes resummed phenomenology for these processes possible. In particular in Ref. [6] results have been presented for the ratio of resummed to unresummed NLO deep–inelastic structure functions. These ratios are shown in Fig. 1 for two choices of the resummed factorization scheme discussed in Ref. [6], and compared to analogous ratio of the fixed order NNLO to NLO. They were determined under the hypothesis that the structure functions F_2 and F_L are kept fixed for all x at $Q_0 = 2$ GeV: this models the situation in which parton distributions are determined at the scale Q_0, and one then sees the change in prediction when going from NLO to NNLO, or from NLO to unresummed. In Sect. 4 we will present evidence for departures from the NLO which appear to be consistent with this figure.

3 Fixed order DGLAP: from HERA to LHC

Fixed–order DGLAP evolution is an integral ingredient of any PDF determination. Currently, the most comprehensive PDF sets are obtained from a global analysis of hard-scattering data from a variety of processes like deep–inelastic scattering, Drell-Yan and weak vector boson production and collider jet production. In such global analysis, QCD factorization and DGLAP evolution are used to relate experimental data to a common set of PDFs. Three groups produce such global analysis and provide regular updates of these: NNPDF [19], CTEQ [20, 21] and MSTW [22]. The typical dataset included in one of such global analysis is shown in Fig. 2. We also show in Fig. 2 the kinematic range which is available at the LHC as compared to that covered by present experimental data: extrapolation to larger Q^2 from the current data region is possible thanks to DGLAP evolution.

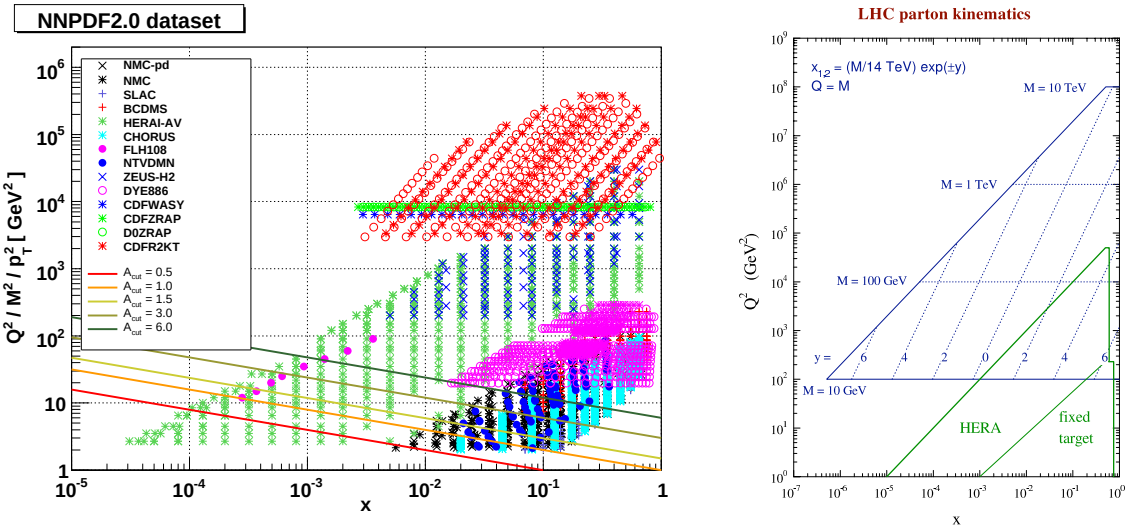

Figure 2: Left: Experimental data used in the NNPDF2.0 global analysis; the series of $A_{\rm cut}$ kinematic cuts is discussed in Sect. 4. Right: LHC kinematical region.

A significant advance in global PDF analysis in the recent years has been the develop-

Fit	2.0 DIS	2.0 DIS+JET	NNPDF2.0
$\chi^2_{\rm tot}$	1.20	1.18	1.21
NMC-pd	0.85	0.86	0.99
NMC	1.69	1.66	1.69
SLAC	1.37	1.31	1.34
BCDMS	1.26	1.27	1.27
HERAI	1.13	1.13	1.14
CHORUS	1.13	1.11	1.18
NTVDMN	0.71	0.75	0.67
ZEUS-H2	1.50	1.49	1.51
DYE605	*7.32*	*10.35*	0.88
DYE866	*2.24*	*2.59*	1.28
CDFWASY	*13.06*	*14.13*	1.85
CDFZRAP	*3.12*	*3.31*	2.02
D0ZRAP	*0.65*	*0.68*	0.47
CDFR2KT	*0.91*	0.79	0.80
D0R2CON	*1.00*	0.93	0.93

Table 1: The χ^2 for individual experiments included in NNPDF2.0 fits with DIS data only, DIS and jet data only, and the full DIS, jet and Drell-Yan data set. For each fit, values of the χ^2 for data not included in the fit are shown in italic. The value of $\chi^2_{\rm tot}$ in the first line does not include these data.

ment of the NNPDF methodology [19, 23–29]. NNPDF provides a determination of PDFs and their uncertainty which is independent of the choice of data set, and which has been shown in benchmark studies [30] to behave in a statistically consistent way when data are added or removed to the fit. Also, because of the use of a Monte Carlo approach, the NNPDF methodology is easily amenable to the use of standard statistical analysis tools. The most updated NNPDF analysis is NNPDF2.0 [19], a global fit to all relevant DIS and hadronic hard scattering data.

Comparing the effect of individual datasets on a global fit such as NNPDF2.0 allows detailed studies of QCD factorization, DGLAP evolution, and the compatibility between DIS and hadronic data. A very stringent test is obtained by comparing the results of a fit to DIS data only to that of DIS+jet data (Table 1). Indeed, it turns out that jet data, which are at much higher scale, are well predicted by PDFs determined from lower scale DIS data. Furthermore, the gluon extracted from the DIS–only fit, which is essentially determined from DGLAP scaling violations, turns out to agree very well with that determined when jet data are also included (see Fig. 3): upon inclusion of the jet data, the uncertainty decreases without a significant change in central value.

Further consistency checks are obtained by comparing the effect of the inclusion of a specific dataset (such as Drell-Yan) to different datasets (such as DIS, or DIS+jets). If there was any inconsistency between different sets, the impact of the new data would be different according to whether they are added to data they are or are not consistent with. No such differences are observed (see Fig. 4). Because the various sets are at different scales and related through DGLAP evolution this also provides a strong check of its accuracy.

4 Deviations from DGLAP in HERA data

We have seen that NLO DGLAP is extremely successful in describing in a consistent way all relevant hard scattering data. On the other hand, there are several theoretical

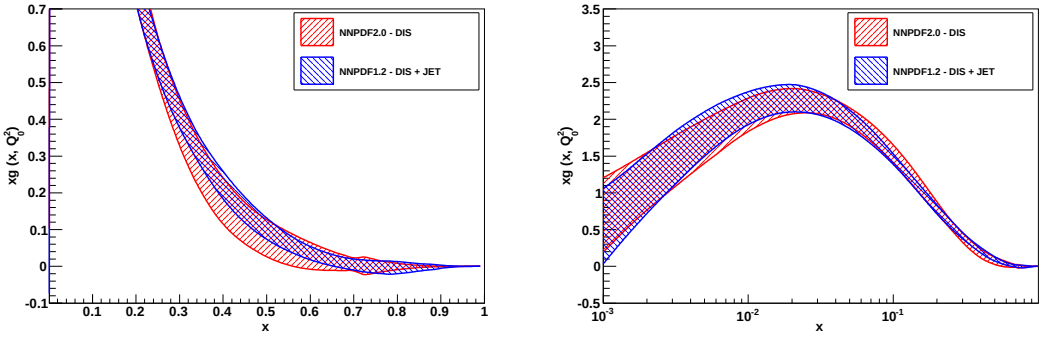

Figure 3: Impact on the gluon distribution of the inclusion of jet data in a fit with DIS data.

indications that at small x and/or at small Q^2 the NLO DGLAP might undergo sizable corrections due to leading–twist small-x perturbative resummation, or non linear evolution, parton saturation and other higher twist effects. Even if it is unclear in which kinematical regime these effects should become relevant, it is likely that eventually they should become relevant, specifically in order to prevent violations of unitarity.

When trying to trace these effects, one should beware of the possibility that putative signals of deviation might in fact be explained using standard NLO theory. An example of this situation is the so–called geometric scaling [31] , which is often thought to provide unequivocal evidence for saturation. This is the prediction, common to many saturation models, that DIS cross sections, at small-x depend only on the single variable

$$\tau(x, Q^2) = \left(Q^2/Q_0^2\right) \cdot (x/x_0)^{\lambda}, \tag{1}$$

rather than on x and Q^2 separately. However, it turns out that geometric scaling Eq. (1) is also generated by linear DGLAP evolution [32]: fixed order DGLAP evolution evolves any (reasonable) boundary condition into a geometric scaling form. Furthermore, the scaling exponent λ Eq. (1) obtained in such way agrees very well with the experimental value.

Following Ref. [32], in Fig. 5 we compare the scaling behaviour of the HERA data and the LO small-x DGLAP evolution of a flat boundary condition: the DGLAP prediction scales even better than data. Note that the accurate combined HERA-I dataset [33] are used here, and that the scaling behaviour persists also at larger $x \lesssim 0.1$, where it is unlikely that it is related to saturation. Clearly, this shows that geometric scaling is not sufficient to conclude that fixed–order DGLAP fails. However, one may wonder whether small-x LO DGLAP is phenomenologically relevant.

To answer this, in Fig. 5 we also show a comparison of the data to the so–called double asymptotic scaling (DAS) [34] form, obtained from the small-x limit of the LO DGLAP solution. The agreement between data and theory is so good that one can see the change in DAS slope when the number of active flavours goes from $n_f = 4$ to $n_f = 5$: so, while on the one hand geometric scaling cannot discriminate between pure DGLAP and saturation, double asymptotic scaling provide evidence that the data follow the predicted DGLAP behavior in most of the HERA region.

However, deviations from DGLAP evolution can be investigated exploiting the more discriminating and sensitive framework of global PDF fits. The key idea in this kind of

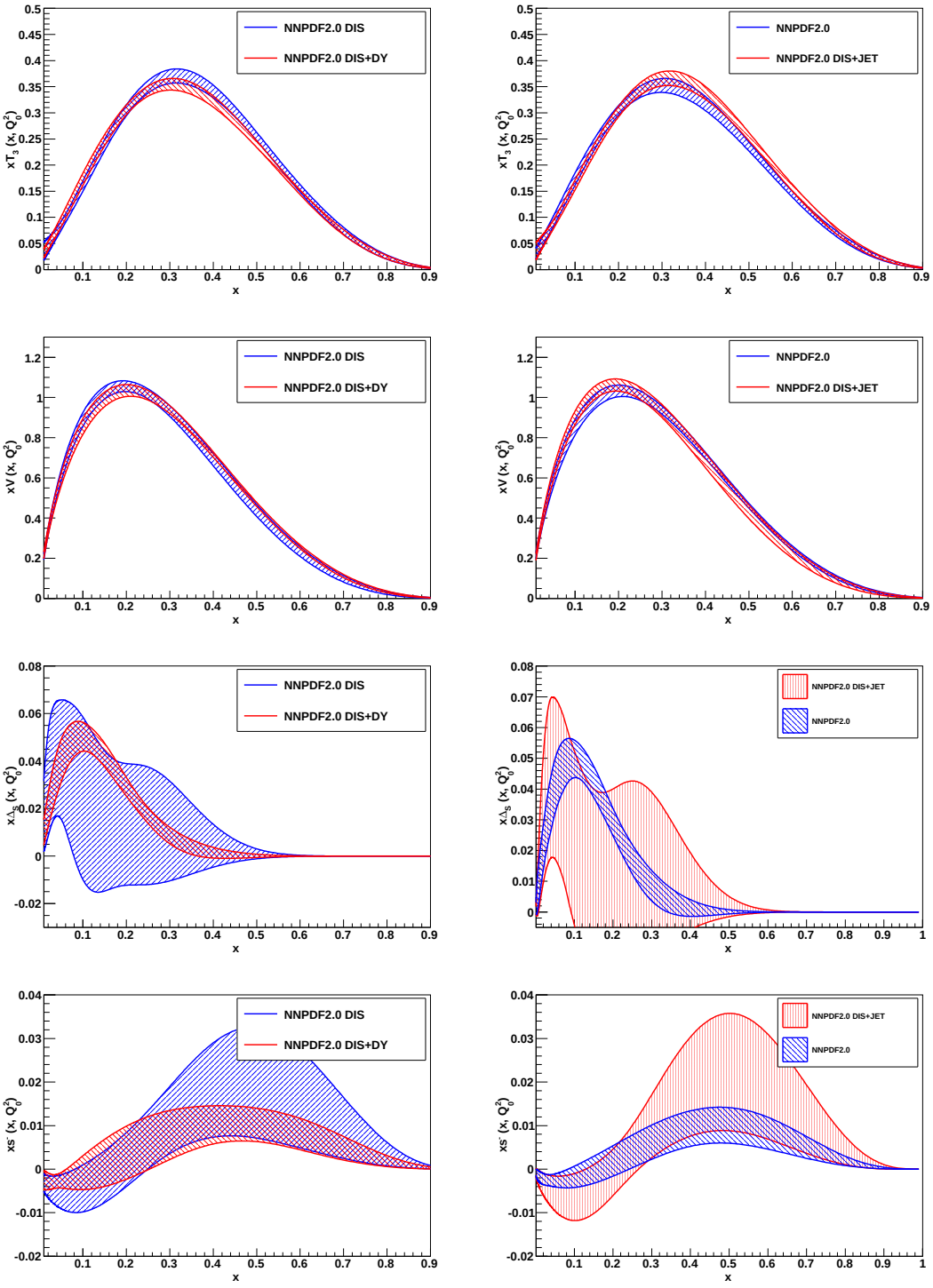

Figure 4: Impact of the inclusion of Drell–Yan data in a fit with DIS data only (left), and in a fit with DIS and jet data (right). From top to bottom, isotriplet, total valence, $\bar{d} - \bar{u}$ and $s - \bar{s}$ PDFs are shown in each case.

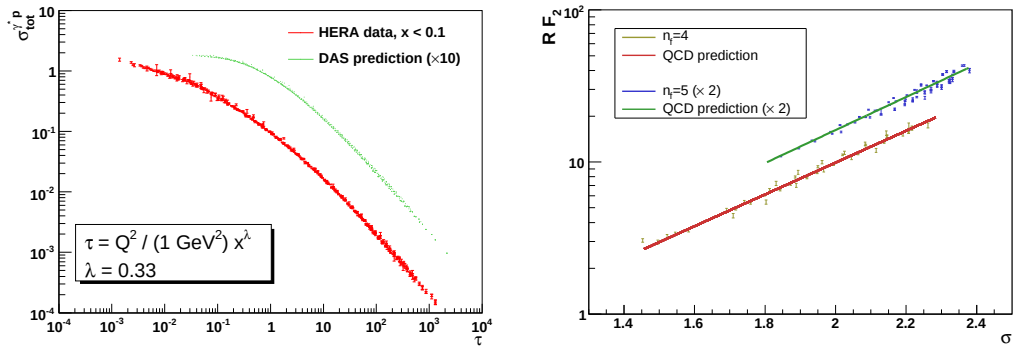

Figure 5: Left: geometric scaling of the HERA-I data and of the (Double Asymptotic Scaling) small–x solution of the LO DGLAP evolution equation for a a flat boundary condition at $Q_0^2 = 1$ GeV^2. Only points with $Q^2 > 10$ GeV^2 are included in the DAS curve, which is offset for clarity. Right: the rescaled proton F_2 structure function plotted as a function of the DAS variables $\sigma \equiv \sqrt{\ln 1/x \ln(\ln t/t_0)}$, with $t = \ln Q^2/\Lambda^2_{QCD}$ and $Q_0 = 1$ GeV. The points correspond to the same data and the curves corresponds to the same prediction as in the right plot. The two curves include data with 10 GeV$^2 \geq Q^2 \geq 25$ GeV^2 and $x < 0.01$ ($n_f = 4$) or $Q^2 \geq 25$ GeV^2 and $x < 0.07$ ($n_f = 5$).

analysis is to perform global fits only in the large-x, large-Q^2 region, where NLO DGLAP is certainly reliable. This way one can determine "safe" parton distributions which are not contaminated by possible non-DGLAP effects. These "safe" PDFs are then evolved backwards into the potentially "unsafe" low-x and low-Q^2 kinematic region, and used to compute physical observables, which are compared with data. A deviation between the predicted and observed behaviour in this region can then provide a signal for effects beyond NLO DGLAP. Since possible deviations are small, this kind of studies is meaningful only on statistical grounds, hence a reliable estimate of PDFs uncertainties and theoretical biases is mandatory. The NNPDF framework provides useful tools for this kind of investigations.

In [35] such an analysis was performed using the NNPDF1.2 PDF set [28], and it did provide some evidence for deviations from NLO DGLAP. Here, we update this analysis using the NNPDF2.0 PDF set discussed in Sect. 3. In comparison to NNPDF1.2, NNPDF2.0 also includes hadronic data (fixed target Drell-Yan production, collider weak boson production and collider inclusive jets), and the combined HERA-I dataset [33] replaces previously less accurate data from ZEUS and H1. The inclusion of the very accurate combined HERA-I dataset has the potential to increase the significance of the observed deviations from DGLAP, while the presence of hadronic data allows stringent tests of the global compatibility of the NLO DGLAP framework, as discussed in Sect. 3. A further difference between NNPDF1.2 and NNPDF2.0 is an improved treatment of normalization uncertainties based on the so–called t_0 method [29], which avoids the biases of other commonly used methods to deal with normalization uncertainties.

The "safe" region, where non–DGLAP effects are likely to be negligible, is defined as

$$Q^2 \geq A_{\rm cut} \cdot x^{\lambda}, \tag{2}$$

with $\lambda = 0.3$. This definition has the feature of only considering unsafe small-x data if their scale is low enough, with the relevant scale raised as x is lowered; its detailed shape

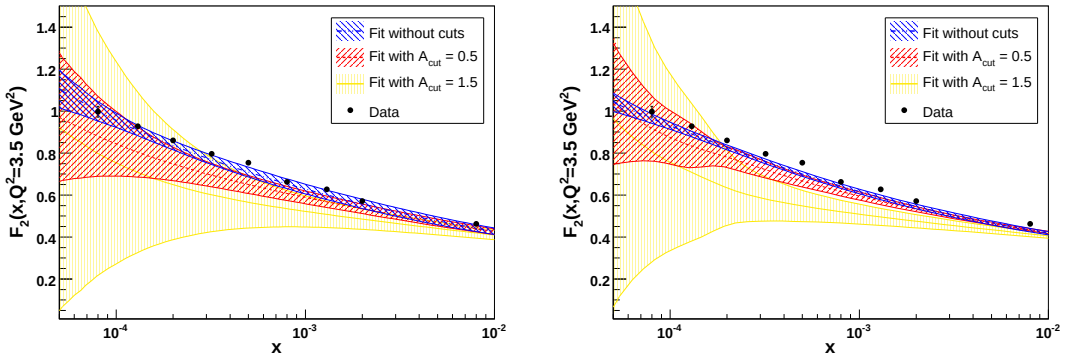

Figure 6: The proton structure function $F_2(x, Q^2)$ computed using NNPDF1.2 (left) or NNPDF2.0 (right) PDFs obtained from fits with different values of $A_{\rm cut}$.

is inspired by saturation and resummation studies. We have performed fits with only data which pass the cut Eq. (2) included, with a variety of choices for $A_{\rm cut}$, shown in Fig. 2. Results depend smoothly on $A_{\rm cut}$.

As a first test, we have computed the proton structure function F_2 and compared it with data (see Fig. 6) at $Q^2 = 3.5$ GeV^2, where a significant x range falls below the cut (compare with Fig. 2). Clearly, the prediction obtained from backward evolution of the data above the cut exhibits a systematic downward trend. This deviation, which becomes more and more apparent as $A_{\rm cut}$ is raised, is visible but marginal when the NNPDF1.2 set based on old HERA data is used, but it becomes rather more significant when using NNPDF2.0 and new HERA data. Interestingly, with old HERA data the uncut fit agrees well with the data, showing that whatever the possible deviation between data and theory, it is absorbed by the PDFs. This is no longer possible when the more precise combined HERA data are used: in such case, even when no cut is applied, the theory cannot reproduce the data fully. This suggests that low-x and Q^2 NLO DGLAP evolution is stronger than the scale dependence seen in the data.

In order to quantify this observed deviation from NLO DGLAP, we introduce the statistical distance

$$d_{\rm stat}(x, Q^2) \equiv \frac{F_{\rm data} - F_{\rm fit}}{\sqrt{\sigma_{\rm data}^2 + \sigma_{\rm fit}^2}}, \tag{3}$$

i.e. the difference between the observable $F_{\rm data}$ and the NLO DGLAP prediction $F_{\rm fit}$ in unit of their combined uncertainties $\sigma_{\rm fit}$, $\sigma_{\rm data}$. Note that $d_{\rm stat} \sim 1$ corresponds to a 1–sigma effect.

In Fig. 7 we plot the statistical distance Eq. (3) between small-x HERA data and the NNPDF1.2 and NNPDF2.0 fits without cuts (i.e. with $A_{\rm cut} = 0$) and with the cut $A_{\rm cut} = 1.5$. Again, we see that with NNPDF1.2 if all data are included the fit manages to compensate for the deviation by readjusting the PDFs: the fit lies both above and below the data and the mean distances is compatible with zero: from the points plotted in Fig. 7 we obtain $\langle d_{stat} \rangle = 0.06 \pm 0.56$. On the other hand using NNPDF2.0, based on the combined HERA-I data, we get $\langle d_{stat} \rangle = 1.1 \pm 0.7$, which shows a systematic tension

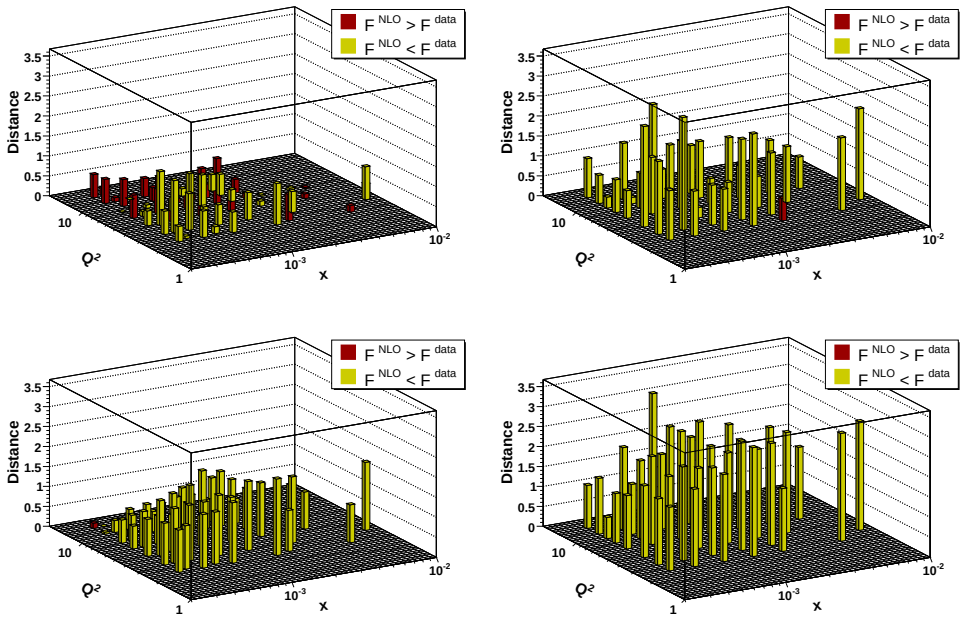

Figure 7: Statistical distance, Eq. (3), between small-x HERA data and NLO DGLAP prediction for fits without kinematical cuts (top row) and fits with the cut at $A_{\rm cut} = 1.5$ (bottom row). Both results obtained using NNPDF1.2 with separate HERA data (left) and NNPDF2.0 with combined HERA data (right) are shown.

at the one-σ level between data and theory. When the cut is applied, the discrepancy is apparent: using NNPDF1.2 $\langle d_{stat} \rangle = 0.95 \pm 0.45$, while with NNPDF2.0 $\langle d_{stat} \rangle = 2.0 \pm 0.7$, i.e. a systematic deviation between data and prediction now at the three-σ level.

It is interesting to note that the significance of the effect is considerably weakened if one instead of performing the cut Eq. (2) were to simply cut out the small-x region at all Q^2. For example, if we consider the region $x \leq 0.01$ we obtain (from HERA-I data only) $\langle d_{stat} \rangle = 1.1 \pm 0.9$ from the global fit ($A_{\rm cut} = 0$) and $\langle d_{stat} \rangle = 1.2 \pm 1.0$ from the fit with maximum cut ($A_{\rm cut} = 1.5$): this shows that indeed it is only at low Q^2 that deviations appear, as one would expect of an effect driven by perturbative evolution. A recent study [36] did find that in the low-x region the distance fluctuations are larger than expected, consistent with our conclusions, but no significant deviation of $\langle d \rangle$ from zero was found in this less sensitive $x \leq 0.01$ region for an uncut fit, also consistent with our conclusion.

Evidence for a systematic deviation between data and theory is also provided by studying the behaviour of the $\left\langle d^2_{stat} \right\rangle$ in different kinematic slices, both without cuts and with $A_{\rm cut} = 1.5$. The results, displayed in Fig. 8, show that data and theory increasingly deviate as one moves towards the small-x, small-Q^2 region. This deviation is already present when all data are fitted, but it becomes significantly stronger when the cut is applied. However, the discrepancy is concentrated in the region which is affected by the cuts. Indeed, in Tab. 2 we compare the χ^2 of various datasets for the cut and uncut fits: the quality of the fit to high–scale hadronic data, unaffected by the cuts, is the same in the two fits.

Having strengthened our previous [35] conclusion that there is evidence for deviations

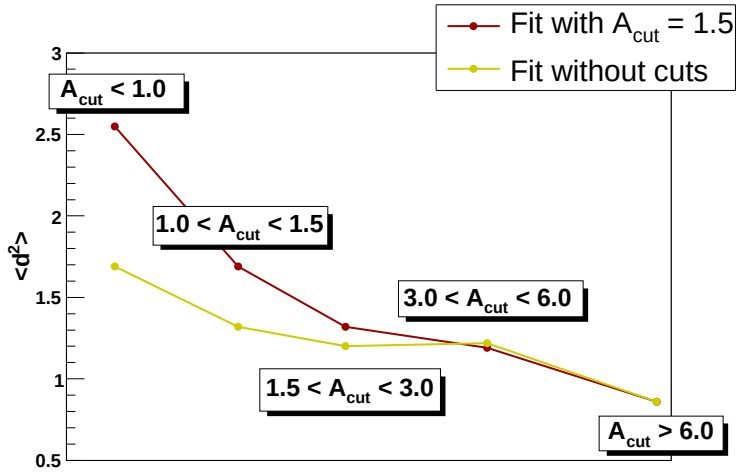

Figure 8: $\langle d^2_{stat} \rangle$ computed in the different kinematic slices of Fig. 2: from the NNPDF2.0 fit without kinematic cuts (yellow, lower curve) and with the $A_{\rm cut} = 1.5$ cut (red, top curve).

Fit	All dataset	Only fitted points
$\chi^2_{\rm tot}$	1.78	1.14
NMC-pd	0.98	0.98
NMC	1.75	1.75
SLAC	1.42	1.42
BCDMS	1.22	1.22
HERAI	4.54	1.04
CHORUS	1.14	1.14
NTVDMN	0.70	0.70
ZEUS-H2	1.23	1.23
DYE605	0.82	0.82
DYE866	1.25	1.25
CDFWASY	1.86	1.86
CDFZRAP	1.85	1.82
D0ZRAP	0.56	0.56
CDFR2KT	0.66	0.66
D0R2CON	0.82	0.82

Table 2: The χ^2 of the individual experiments included in NNPDF2.0 for the $A_{\rm cut} = 1.5$ fit. Col. 2 shows χ^2 computed on all NNPDF2.0 dataset, while Col. 3 the χ^2 computed only on data which pass the cut.

from NLO DGLAP evolution in small-x and Q^2 HERA data one may ask what are possible theoretical explanations for the observed effect. Because NLO DGLAP overestimates the amount of evolution required to reproduce experimental data, NNLO corrections as a possible explanation are ruled out, as they would lead to yet stronger evolution in this region thus making the discrepancy larger. This conclusion was recently confirmed by the HERAPDF group, which finds that the description of small-x and Q^2 HERA-I data worsens when NNLO corrections are included [37]. Charm mass effects, not included in NNPDF2.0, could be partly responsible, but they seem [35] too small to account for the data. This conclusion is borne out by preliminary studies based on the NNPDF2.1 set [18] which does include charm mass effects using the FONLL [38, 39] framework, and which confirm the conclusions of the present study.

Interestingly, the small-x resummation corrections shown in Fig. 1 and discussed in Sect. 2 go in the right direction, and appear to be roughly of the size which is needed to explain the data. A quantitative confirmation that this is actually the case could come from a fully resummed PDF fit, which is doable using current knowledge and it would only require implementation of the resummation in a PDF fitting code. An alternative interesting possibility is that the observed slow-down of perturbative evolution may be due to saturation effects related to parton recombination. However, it is more difficult to single out a clear signature for these effects, given that saturation models usually yield predictions for the x dependence of structure functions, rather than their scale dependence which is relevant in this context.

Finally, one may ask whether these deviations, if real, might bias LHC phenomenology. A first observation is that these deviations might explain the well–known fact [1] that the α_s value obtained from deep–inelastic scattering tends to be lower that the global average: if the observed evolution is weaker than the predicted one, the value of the coupling is biased downwards: the value of α_s from a fully resummed fit would be higher. A more direct impact on HERA phenomenology can be assessed by comparing predictions for LHC standard candles obtained from cut and uncut fits: their difference provides a conservative upper bound for the phenomenological impact of these deviations. In Table 3 we show results for W, Z, Higgs and $t\bar{t}$ inclusive production at the LHC at 7 TeV center of mass energies, computed with the MCFM code [40]. Even with the largest kinematical cuts, $A_{\rm cut} = 1.5$, the corrections are moderate, below the 1–sigma level (except for $t\bar{t}$), of similar size of other comparable effects at the precision level, such as α_s uncertainties [41] or variations of the charm mass.

The impact of the effect we discovered is moderate at present but it might become significant as the accuracy of PDF determination improves. It will be interesting to see whether further confirmation of the effect comes from other groups. Its full understanding might lead to a deeper grasp of perturbative QCD.

The NNPDF2.0 PDFs (sets of $N_{\rm rep} = 100$ and 1000 replicas) and the PDF sets based on NNPDF2.0 with various $A_{\rm cut}$ kinematical cuts are available at the NNPDF web site,

Observable	NNPDF2.0 without cuts	NNPDF2.0 with $A_{\rm cut} = 1.5$
$\sigma(W^+)\mathrm{B}_{l^+\nu}$ [nb]	5.80 $\pm$ 0.09	5.87 $\pm$ 0.13
$\sigma(W^-)\mathrm{B}_{l^-\bar{\nu}}$ [nb]	3.97 $\pm$ 0.06	4.01 $\pm$ 0.07
$\sigma(Z)\mathrm{B}_{l^+l^-}$ [nb]	2.97 $\pm$ 0.04	2.98 $\pm$ 0.05
$\sigma(t\bar{t})$ [pb]	169 $\pm$ 5	160 $\pm$ 7
$\sigma(H, m_H = 120$ GeV) [pb]	11.60 $\pm$ 0.15	11.53 $\pm$ 0.25

Table 3: LHC observables at 7 TeV computed from the default NNPDF2.0 set and with the fit with kinematical cut $A_{\rm cut} = 1.5$ using MCFM [40]. All PDF uncertainties are 1–sigma.

`http://sophia.ecm.ub.es/nnpdf .`

NNPDF2.0 is also available through the LHAPDF interface [42].

References

[1] G. Altarelli, In *Landolt-Boernstein I 21A: Elementary particles* 4.

[2] S. Catani, M. Ciafaloni and F. Hautmann, Nucl. Phys. B366 (1991) 135.

[3] S. Catani and F. Hautmann, Nucl. Phys. B427 (1994) 475, hep-ph/9405388.

[4] G. Altarelli, R.D. Ball and S. Forte, Nucl. Phys. B674 (2003) 459, hep-ph/0306156.

[5] G. Altarelli, R.D. Ball and S. Forte, Nucl. Phys. B742 (2006) 1, hep-ph/0512237.

[6] G. Altarelli, R.D. Ball and S. Forte, Nucl. Phys. B799 (2008) 199, 0802.0032.

[7] M. Ciafaloni et al., Phys. Rev. D68 (2003) 114003, hep-ph/0307188.

[8] M. Ciafaloni et al., Phys. Lett. B587 (2004) 87, hep-ph/0311325.

[9] M. Ciafaloni et al., JHEP 08 (2007) 046, 0707.1453.

[10] R.D. Ball and R.K. Ellis, JHEP 05 (2001) 053, hep-ph/0101199.

[11] S. Marzani et al., Nucl. Phys. B800 (2008) 127, 0801.2544.

[12] S. Marzani et al., Nucl. Phys. Proc. Suppl. 186 (2009) 98, 0809.4934.

[13] S. Marzani and R.D. Ball, Nucl. Phys. B814 (2009) 246, 0812.3602.

[14] S. Marzani and R.D. Ball, (2009), 0906.4729.

[15] G. Diana, Nucl. Phys. B824 (2010) 154, 0906.4159.

[16] G. Diana, J. Rojo and R.D. Ball, (2010), 1006.4250.

[17] R.D. Ball, Nucl. Phys. B796 (2008) 137, 0708.1277.

[18] J. Rojo et al., (2010), 1007.0354.

[19] R.D. Ball et al., Nucl. Phys. B838 (2010) 136, 1002.4407.

[20] P.M. Nadolsky et al., Phys. Rev. D78 (2008) 013004, 0802.0007.

[21] H.L. Lai et al., (2010), 1004.4624.

[22] A.D. Martin et al., Eur. Phys. J. C63 (2009) 189, 0901.0002.

[23] S. Forte et al., JHEP 05 (2002) 062, hep-ph/0204232.

[24] The NNPDF Collaboration, L. Del Debbio et al., JHEP 03 (2005) 080, hep-ph/0501067.

[25] The NNPDF Collaboration, L. Del Debbio et al., JHEP 03 (2007) 039, hep-ph/0701127.

[26] The NNPDF Collaboration, R.D. Ball et al., Nucl. Phys. B809 (2009) 1, 0808.1231.

[27] The NNPDF Collaboration, J. Rojo et al., (2008), 0811.2288.

[28] The NNPDF Collaboration, R.D. Ball et al., Nucl. Phys. B823 (2009) 195, 0906.1958.

[29] The NNPDF Collaboration, R.D. Ball et al., JHEP 05 (2010) 075, 0912.2276.

[30] M. Dittmar et al., (2009), 0901.2504.

[31] A.M. Stasto, K.J. Golec-Biernat and J. Kwiecinski, Phys. Rev. Lett. 86 (2001) 596, hep-ph/0007192.

[32] F. Caola and S. Forte, Phys. Rev. Lett. 101 (2008) 022001, 0802.1878.

[33] H1, F.D. Aaron et al., JHEP 01 (2010) 109, 0911.0884.

[34] R.D. Ball and S. Forte, Phys. Lett. B335 (1994) 77, hep-ph/9405320.

[35] F. Caola, S. Forte and J. Rojo, Phys. Lett. B686 (2010) 127, 0910.3143.

[36] H.L. Lai et al., (2010), 1007.2241.

[37] A. Cooper-Sarkar, http://indico.cern.ch/conferenceDisplay.py?confId=98883, 2010.

[38] S. Forte et al., Nucl. Phys. B834 (2010) 116, 1001.2312.

[39] SM and NLO Multileg Working Group, J.R. Andersen et al., (2010), 1003.1241.

[40] J.M. Campbell and R.K. Ellis, Phys. Rev. D62 (2000) 114012, hep-ph/0006304.

[41] F. Demartin et al., Phys. Rev. D82 (2010) 014002, 1004.0962.

[42] D. Bourilkov, R.C. Group and M.R. Whalley, (2006), hep-ph/0605240.